Science World Journal Vol. 20(No 4) 2025 https://dx.doi.org/10.4314/swj.v20i4.44
www.scienceworldjournal.org
ISSN: 1597-6343 (Online), ISSN: 2756-391X (Print)
Published by Faculty of Science, Kaduna State University

Full Length Research Article

HYBRID OPTICAL PROPERTIES OF GaAs QUANTUM DOTS

[1]Teslim A. Alabi, [1]I.C. Ndukwe, [1]C.P. Onyenegecha, *[2]Ibeabuchi E. Okwor

[1]Department of Physics, Federal University of Technology, P.M.B. 1526, Owerri, Imo State, Nigeria
[2]David Umahi Federal University of Health Sciences, P.M.B 211, Uburu, Ebonyi State, Nigeria

*Corresponding Author Email Address: okworie@dufuhs.edu.ng

ABSTRACT
The study presents results of the linear and non-linear optical properties of GaAs quantum dots. The reported work aims to provide new results of the quantum dot optical properties confined in Hua plus modified Eckart (HPME) potential. To obtain analytical expressions for the energy eigenvalues and the wave functions, we solved the time-independent Schrödinger equation for the HPME potential by using the parametric Nikiforov-Uvarov (NU) method. Investigation of the linear, third-order nonlinear, and total absorption coefficients and refractive index changes was done with the help of the density matrix approach. The results showed that the energy decreases in a linear manner as the potential parameter, *V0*. Also, it is observed that as the barrier slope increases, the peaks of the linear, third-order linear, and total absorption coefficient tend to higher values of energy. Furthermore, as the barrier slope increases, the change in refractive indices increases, and their positions shift to higher energies. Additionally, an increase in the structure parameters and optical intensity greatly influences the absorption coefficients and the refractive index changes of the quantum dots.

Keywords: Optical Properties; Quantum dot; Schrödinger equation; Nikiforov-Uvarov method; Density matrix method

INTRODUCTION

Low-dimensional structures (LDS) have been a central area of research for many years. They are semiconductor materials, with scale in one or two dimensions, such that they have electronic properties that clearly differ from the same bulk material. These properties are altered by the effects of quantum mechanics. All over the world, increasing research time has been devoted to the preparation, study, and application of low-dimensional structures. Investigation into these structures has aggressively transformed the science of condensed matter, particularly semiconductor-related materials. The complex nature of LDS offers scientists and engineers better insights and opportunities to design tunable, generation photonic and electronic devices. The wizardry of modern fabrication methods such as molecular beam epitaxy (MBE) and metal–organic chemical vapour (MOCVD) deposition has now led to the possibility of creating such low-dimensional structures in reality and practice. These advanced techniques used to grow high-quality epitaxial layers of semiconductors on semiconductor crystal substrates are increasingly becoming very crucial for the advancement of the semiconductor electronics industry.

Currently, quantum wells (QW), quantum wires (QWR), and quantum dots (QD) are the most commonly studied LDS. Quantum dots (QD) are nanostructures that are quantum confined in 3 dimensions, which results in many peculiar and useful optical and transport properties. Quantum Confinement is the spatial confinement/entrapment of pairs of electrons and holes in one or more dimensions within a material. Charge carrier confinement in QDs happens in three directions. In low-temperature physics, impurity influences many physical properties, such as optical and transport phenomena. Due to the fact that semiconductors have a band gap in their electronic band structure, quantum confinement is observed more in semiconductors. Metals do not have a band gap; therefore, quantum confinement is less obvious. To observe quantum confinement, the dimensions have to be below 2 nm. Since the beginning of the quantum theory, the study of quantum confinement has been one of the most interesting subjects of research. The research interest in the physical properties of quantum confined structures like quantum wells (1- dimensional confinement), quantum wires (2-dimensional confinement), and QDs (3-dimensional confinement), has become more significant, with the recent progress in semiconductor nanotechnology (Theerapong *et al*., 2008; Tomoaki *et al*., 2008; Xiang-Hong *et al.*, 1998). Due to quantum size effects in these structures, atomic-like discrete energy levels (sub-bands) are formed, in contrast to the energy bands in bulk crystals.

A lot of attention has been drawn to semiconductor quantum dot (QD) structures because of their peculiar physical properties and their potential applications in micro and optoelectronic devices (Ataser *et al*., 2018; Bhattacharya *et al*., 2004; Kang *et al.*, 2015; Karimkhani & Moravvej-Farsh, 2010; Rishinaramangalam *et al*., 2015; Teleb *et al*., 2011), life sciences and biotechnology (Jorge *et al*., 2006; Liang *et al*., 2006), thermoelectrics (Pennelli, 2015; Cecchi *et al.*, 2015). Semiconductor QDs have potential applications in various optoelectronic devices, in biological labeling, in light-emitting diodes (LEDs), detectors, etc. They also have applications in solar cells as a result of their relatively higher efficiency compared to bulk semiconductors (Ataser *et al*., 2018; Ee *et al.*, 2008; Jorge *et al.*, 2006; Liang *et al.*, 2006; Luque *et al.*, 2010). In zero-dimensional structures, the free carriers are entrapped in a tiny region by a confinement potential that provides the quantization of electronic energy states dependent on the size of the dots. Recently, the optical properties of spherical quantum dots have been reported theoretically (Mathe *et al.*2021; Onyeaju & Onate, 2020; Onyenegecha, 2022; Tshipa, 2019). The optical properties, such as index refraction, coefficient of absorption, and absorption cross section, can be determined easily once the linear and nonlinear susceptibilities of the QD are known. The nonlinear contribution of the dielectric constant is enhanced by large electric dipole matrix elements coupled with small energy differences between subbands, so one expects that the intensity of light plays an important part in the optical properties of the QDs. Hence, the size of dots can influence the values of electronic energy eigenvalues and their corresponding envelope functions.

MATERIALS AND METHODS

The Schrödinger equation is a fundamental wave equation in physics; it is essential for understanding the nature and behavior of

particles in quantum systems. One of the fundamental challenges in quantum mechanics is to determine exact solutions to the Schrödinger equation in bound states for potentials of considerable interest. These solvable potentials are very vital to successfully implement approximate methods in studying physical systems. Different techniques applied by various authors to obtain the exact solutions of the Schrodinger equations in bound states with non-central potentials are the standard approach (Zhang & Guo, 2010), the path integral approach (Chetouani *et al*, 1987), the Nikiforov-Uvarov method (Onyenegecha, 2022; Ikhdair, 2008; Antia *et al*, 2010), the supersymmetric technique (Gonul & Zorba, 2000), amongst others.

In this work, the methods we have adopted are purely theoretical approaches based on the quantum mechanical principles of the parametric Nikiforov-Uvarov method and the Density Matrix techniques. These methods are briefly described, as well as their specific use and applications in this work.

Schrodinger Equation in Spherical Coordinates

The time-independent Schrodinger equation describing the particle's behaviour in a quantum system is given by eq. (1).

$$-\frac{\hbar^2}{2\mu}\nabla^2\psi(r)+V(r)\psi(r) = E\psi(r), \quad (1)$$

where ∇^2 is the Laplacian in the form of spherical coordinates

$$\nabla^2 = \frac{1}{r^2}\frac{\partial}{\partial r}\left(r^2\frac{\partial}{\partial r}\right)+\frac{1}{r^2\sin\theta}\frac{\partial}{\partial\theta}\left(\sin\theta\frac{\partial}{\partial\theta}\right)+\frac{1}{r^2\sin^2\theta}\frac{\partial^2}{\partial\phi^2} \quad (2)$$

Substituting equation (2) into equation (1) produces the Schrodinger equation in spherical coordinates as

$$-\frac{\hbar^2}{2\mu}\left[\frac{1}{r^2}\frac{\partial}{\partial r}\left(r^2\frac{\partial}{\partial r}\right)+\frac{1}{r^2}\frac{1}{\sin\theta}\frac{\partial}{\partial\theta}\left(\sin\theta\frac{\partial}{\partial\theta}\right)+\frac{1}{r^2\sin^2\theta}\frac{\partial^2}{\partial\varphi^2}\right]\Psi(r,\theta,\varphi)+V(r)\Psi(r,\theta,\varphi) = E\Psi(r,\theta,\varphi) \quad (3)$$

where $E, \hbar, \mu$ and Ψ are respectively the energy, reduced Planck constant, reduced mass, and wave function of the system.

Choosing $\Psi(r,\theta,\phi)=\frac{R(r)}{r}\psi_{nl}(\theta,\phi)$ as the solution to (3), the radial part of the Schrodinger equation with the centrifugal term is obtained as

$$\frac{d^2R_{nl}(r)}{dr^2}+\left[\frac{2\mu}{\hbar^2}\left(E_{nl}-V(r)\right)-\frac{l(l+1)}{r^2}\right]R_{nl}(r)=0, \quad (4)$$

where n is the radial quantum number and l the orbital angular momentum quantum number.

The Parametric Nikiforov- Uvarov Technique

The Nikiforov–Uvarov (NU) method was applied in obtaining the solutions of hypergeometric second-order differential equations using special orthogonal functions (Nikiforov & Uvarov, 1988). Due to the fact that the conventional form of this method is very tedious, Tezcan & Sever, 2009 derived a simpler parametric form of the NU method. To use the parametric form of the NU method, we considered a general second-order differential equation of the form:

$$\frac{d^2\psi(s)}{ds^2}+\frac{\alpha_1-\alpha_2 s}{s(1-\alpha_3 s)}\frac{d\psi(s)}{ds}+\frac{-\xi_1 s^2+\xi_2 s-\xi_3}{s^2(1-\alpha_3 s)^2}\psi(s)=0 \quad (5)$$

The energy and wave functions are obtained from (6) and (7), respectively.

$$(\alpha_2-\alpha_3)n+\alpha_3 n^2-(2n+1)\alpha_5+(2n+1)\left(\sqrt{\alpha_9}+\alpha_3\sqrt{\alpha_8}\right)+\alpha_7+2\alpha_3\alpha_8+2\sqrt{\alpha_8\alpha_9}=0, \quad (6)$$

$$\psi(s)=N_{nl}s^{\alpha_{12}}(1-\alpha_3 s)^{-\alpha_{12}-\left(\frac{\alpha_{13}}{\alpha_3}\right)}P_n^{\left(\alpha_{10}-1,\frac{\alpha_{11}}{\alpha_3}-\alpha_{10}-1\right)}(1-2\alpha_3 s) \quad (7)$$

where

$$\left.\begin{aligned}&\alpha_4=\tfrac{1}{2}(1-\alpha_1),\alpha_5=\tfrac{1}{2}(\alpha_2-2\alpha_3),\alpha_6=\alpha_5^2+\xi_1,\alpha_7=2\alpha_4\alpha_5-\xi_2,\alpha_8=\alpha_4^2+\xi_3,\\&\alpha_9=\alpha_3\alpha_7+\alpha_3^2\alpha_8+\alpha_6,\alpha_{10}=\alpha_1+2\alpha_4+2\sqrt{\alpha_8},\alpha_{11}=\alpha_2-2\alpha_5+2\left(\sqrt{\alpha_9}+\alpha_3\sqrt{\alpha_8}\right)\\&\alpha_{12}=\alpha_4+\sqrt{\alpha_8},\alpha_{13}=\alpha_5-\left(\sqrt{\alpha_9}+\alpha_3\sqrt{\alpha_8}\right)\end{aligned}\right\}, \quad (8)$$

and P_n is the orthogonal Jacobi polynomial defined as

$$P_n^{(\theta,\varphi)}(\omega)=\frac{\Gamma(n+\theta+1)}{n!\Gamma(\theta+1)^2}F_1\left(-n,\theta+\varphi+n+1,\theta+1;\frac{1-\omega}{2}\right).$$

The parametric form of the NU method was the method used in this work to determine the bound states of the Schrodinger equation for the Hua plus modified Eckart (HPME) potential.

Density Matrix Method

Once the energy eigenvalues and the associated eigenfunctions of the Schrödinger equation are obtained, the next step is to determine the optical properties of the system. In principle, the macroscopic optical properties of a system can be properly described based on the density matrix techniques of quantum mechanics, which is a combination of the theory of perturbation with the method of statistical mechanics. Using the density matrix approach, optical properties are investigated starting from the microscopic response of an individual molecule to the applied optical field (Gibbs, 1985; Smith, 1986). The approach has two advantages. Firstly, the mathematical step is clear, simple, and easy to follow. Secondly, both the expectation value of physical quantity for an individual molecule and the macroscopic average of the same quantity for an ensemble of a large number of molecules can be obtained (Gibbs, 1985; Smith, 1986).

Theory of the Density Matrix Method

For a medium with an applied optical field under consideration, and assuming that the Hamiltonian (energy) operator of a whole system is H and that the density matrix operator that describes the physical state of the system is ρ, the time change of the density matrix obeys the following equation:

$$\frac{d\rho}{dt} = -\frac{i}{\hbar}[H\rho-\rho H], \quad (9)$$

where $\hbar$ is Planck's constant divided by 2π. For the conditions

https://dx.doi.org/10.4314/swj.v20i4.44

of resonance, the effect of damping should be considered, and the above equation can be modified as

$$i\hbar\frac{d\rho(t)}{dt} = [H,\ \rho(t)] + i\hbar\left[\frac{d\rho}{dt}\right]_{relaxation}, \quad (10)$$

where the first term on the right-hand side of the equation is expressed by the Poisson brackets, the second term is the phenomenological damping effect.

The total system Hamiltonian is composed of two parts, i.e.,

$$H = H_0 + H'(t), \quad (11)$$

where H_0 is the Hamiltonian (unperturbed) of the medium in the absence of an applied field, and $H'(t)$ is the Hamiltonian of interaction between the medium and the applied optical field. In the case of perturbation, the density matrix operator can be expressed in series form:

$$\rho(t) = \rho^{(0)} + \rho^{(1)}(t) + \rho^{(2)}(t) + \ldots\ldots\ldots + \rho^{(r)}(t) \quad (12)$$

Here, $\rho^{(0)}$ is the initial value of the density matrix when there is no external field, and $\rho^{(r)}(t)$ is the rth term that is assumed to be proportional to the power of $H'(t)$.

Substituting Equations (11) and (12) into Equation (10) gives

$$i\hbar\frac{d\rho^{(1)}}{dt} = [H_0, \rho^{(r)}] + [H', \rho^{(0)}] + i\hbar\Gamma\rho^{(1)} \quad (13)$$

$$i\hbar\frac{d\rho^{(r)}}{dt} = [H_0, \rho^{(r)}] + [H', \rho^{(r-1)}] + i\hbar\Gamma\rho^{(r)} \quad (14)$$

Here $i\hbar\Gamma\rho^{(r)}$ is the relaxation term, which represents the damping effect and Γ is a phenomenological constant due to electron-phonon interaction, electron collisions, etc.

From Equation (14), it is clear that if $\rho^{(0)}$ and $H'(t)$ are known, the solutions from $\rho^{(1)}$ to $\rho^{(r)}$ can be derived by applying a step-by-step method. Finally, the overall density matrix operator ρ can be determined.

For a system under the influence of an electromagnetic field of frequency w such as

$$E(t) = E_0\cos(wt) = \tilde{E}e^{iwt} + \tilde{E}^*e^{-iwt} \quad (15)$$

The time change of the matrix elements of the density operator, ρ, is simply denoted as (Karabulut *et al*, 2006)

$$\frac{\partial\rho}{\partial t} = \left(\frac{1}{i\hbar}\right)[H_0 - qxE(t),\ \rho] - \Gamma(\rho - \rho^{(0)}), \quad (16)$$

Equation (16) can be simplified by adopting the iterative procedure (Ahn & Chuang, 1987b; Khordad, 2013).

$$\rho(t) = \sum_n \rho^{(n)}(t) \quad (17)$$

with

$$\frac{\partial\rho_{ij}^{(n+1)}}{\partial t} = \frac{1}{i\hbar}\left\{[H_0, \rho^{(n+1)}]_{ij} - i\hbar\Gamma_{ij}\rho_{ij}^{(n+1)}\right\} - \frac{1}{i\hbar}[qx, \rho^{(n)}]_{ij}E(t) \quad (18)$$

For a two-level system, the system polarization $\rho(t)$ due to the electric field $\tilde{E}$ can be written as

$$\rho(t) = \varepsilon_0\chi(\omega)\tilde{E}e^{-i\omega t} + \varepsilon_0\chi(-\omega)\tilde{E}^*e^{i\omega t} = \left(\frac{1}{V}\right)Tr(\rho M), \quad (19)$$

where, ρ and V are the electron density matrix and system volume, ε_0 is the free space permittivity, Tr (trace) is the summation over the matrix diagonal elements.

Numerical Results

The results of this study were computed, and plots were made using MATLAB and Maple software.

RESULTS AND DISCUSSION

This section presents the solutions to the Schrodinger equation with Hua plus modified Eckart (HPME) potential. Ikot *et al*. (2015) gave the expression for HPME potential as

$$V(r) = V_0 + V_1\left(\frac{1-e^{-2\alpha r}}{1-qe^{-2\alpha r}}\right)^2 + V_2\left[\frac{4e^{-2\alpha r}}{(1-qe^{-2\alpha r})}\right] + V_3\left[\frac{1+e^{-2\alpha r}}{1-e^{-2\alpha r}}\right] \quad (20)$$

where the parameters V_0, V_1, V_2, V_3, α and q are constants.

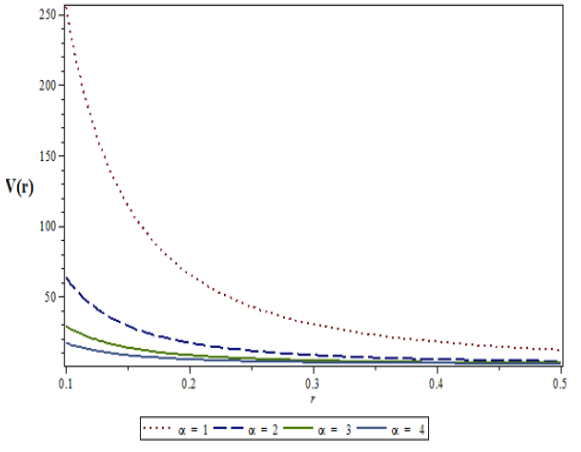

Figure. 1. A plot of HPME potential as a function of r for various values of α

Solutions to the Radial Form of the Schrodinger Equation

To obtain the eigenvalues and associated eigenfunctions of the radial part of the Schrodinger equation, we substitute equation (20)

Science World Journal Vol. 20(No 4) 2025 https://dx.doi.org/10.4314/swj.v20i4.44
www.scienceworldjournal.org
ISSN: 1597-6343 (Online), ISSN: 2756-391X (Print)
Published by Faculty of Science, Kaduna State University

into equation (4) to have

$$\frac{d^2R}{dr^2}+\frac{2m}{\hbar^2}\left[E-V_0-V_1\left(\frac{1-e^{-2\alpha r}}{1-qe^{-2\alpha r}}\right)^2-\frac{4V_2e^{-2\alpha r}}{(1-qe^{-2\alpha r})}-V_3\frac{(1+e^{-2\alpha r})}{(1-qe^{-2\alpha r})}-\frac{l(l+1)}{r^2}\right]R(r)=0 \quad (21)$$

It is important to note here that the exact solution to equation (21) does not exist for $l \neq 0$ as a result of the centrifugal barrier. However, approximate solutions exist.

The first step in achieving the approximate solution to equation (21) starts with the use of the approximation scheme given by Greene & Aldrich (1976) as written below,

$$\frac{1}{r^2}=\frac{4\alpha^2e^{-\alpha r}}{(1-qe^{-2\alpha r})}, \quad (22)$$

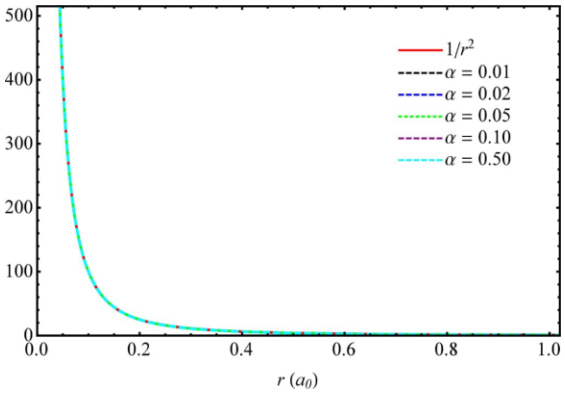

Figure 2: Approximations to the centrifugal barrier

Substituting Eq. (22) into Eq. (21) leads to

$$\frac{d^2R}{dr^2}+\frac{2m}{\hbar^2}\left[E-V_0-V_1\left(\frac{1-e^{-2\alpha r}}{1-qe^{-2\alpha r}}\right)^2-\frac{4V_2e^{-2\alpha r}}{(1-qe^{-2\alpha r})}-V_3\frac{(1+e^{-2\alpha r})}{(1-qe^{-2\alpha r})}-\frac{4\alpha^2e^{-\alpha r}l(l+1)}{(1-qe^{-2\alpha r})^2}\right]R(r)=0 \quad (23)$$

By making use of Equation (8), we obtain the constants,

$$\left.\begin{aligned}
&\alpha_1=\alpha_2=\alpha_3=1\\
&\alpha_4=0,\alpha_5=-\frac{1}{2}\\
&\alpha_6=\frac{1}{4}+\varepsilon^2+\frac{V_1}{4\alpha^2q}-\frac{V_2}{\alpha^2q}-\frac{V_3}{4\alpha^2q}\\
&\alpha_7=-\left(2\varepsilon^2+\frac{2V_1}{4\alpha^2}-\frac{V_2}{\alpha^2q}-\frac{V_3(1-q)}{4\alpha^2q}-\frac{\lambda}{q}\right)\\
&\alpha_8=\varepsilon^2+\frac{V_1q+V_3}{4\alpha^2}.
\end{aligned}\right\} \quad (24)$$

Other parameters obtained from equations (8) are:

$$\left.\begin{aligned}
&\alpha_9=\frac{1}{4}-\frac{2V_1+V_1q}{4\alpha^2}+\frac{V_1}{4\alpha^2q}+\frac{\lambda}{q}\\
&\alpha_{10}=1+2\sqrt{\varepsilon^2+\frac{V_1q+V_3}{4\alpha^2}}\\
&\alpha_{11}=2+2\left(\sqrt{\frac{1}{4}+\frac{V_1q-2V_1}{4\alpha^2}+\frac{V_1}{4\alpha^2q}+\frac{\lambda}{q}}+\sqrt{\varepsilon^2+\frac{V_1q-V_3}{4\alpha^2}}\right)\\
&\alpha_{12}=\sqrt{\varepsilon^2+\frac{V_1q+V_3}{4\alpha^2}}\\
&\alpha_{13}=-\frac{1}{2}-\left(\sqrt{\frac{1}{4}+\frac{V_1q-2V_1}{4\alpha^2}}+\frac{V_1}{4\alpha^2q}+\frac{\lambda}{q}+\sqrt{\varepsilon^2+\frac{V_1q+V_3}{4\alpha^2}}\right)
\end{aligned}\right\} \quad (25)$$

Substituting (24) and (25) into Equation (6) and carrying out some mathematical simplification gives the equation for the energy eigenvalues of the HPME potential as given below:

$$E=V_0+\frac{V_1q\hbar^2+V_3\hbar^2}{4m}+\frac{\alpha^2\hbar^2}{m}\left[\frac{(n+\sigma)^2+\Omega}{2(n+\sigma)}\right]^2 \quad (26)$$

where,

$$\sigma=\frac{1}{2}\sqrt{\frac{1}{4}+\frac{V_1(q-2)}{4\alpha^2}+\frac{V_1}{4\alpha^2q}+\frac{\lambda}{q}}$$

$$\Omega=\frac{V_2}{\alpha^2q}+\frac{V_3-V_1}{4\alpha^2q}+\frac{V_1q}{2\alpha^2}-\frac{(V_3+V_1q)}{4\alpha^2}$$

Science World Journal Vol. 20(No 4) 2025 https://dx.doi.org/10.4314/swj.v20i4.44
www.scienceworldjournal.org
ISSN: 1597-6343 (Online), ISSN: 2756-391X (Print)
Published by Faculty of Science, Kaduna State University

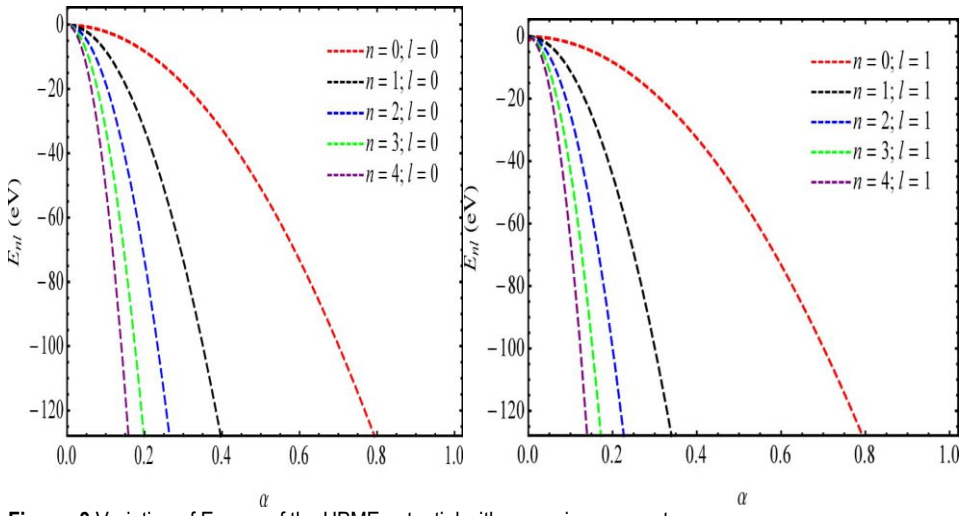

Figure. 3 Variation of Energy of the HPME potential with screening parameter

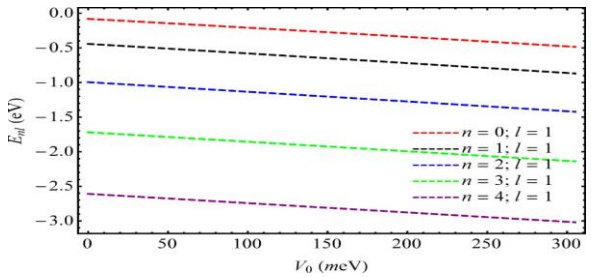

Figure 4 Variation of the energy with the barrier height for various quantum number *n* and α = 0.02

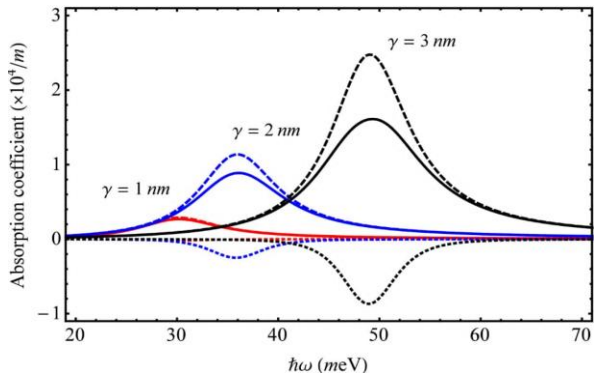

Figure 5 Variation of Linear (dashed line), third-order nonlinear (dotted line), and total absorption (solid line) coefficients incident photon energy for three different values of confinement barrier slope

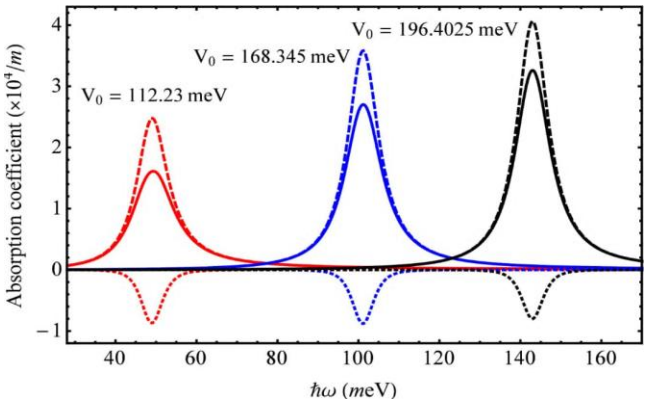

Figure 6 Variation of Linear (dashed line), third-order nonlinear (dotted line), and total absorption (solid line) coefficients with incident photon energy for three different values of barrier height V_0

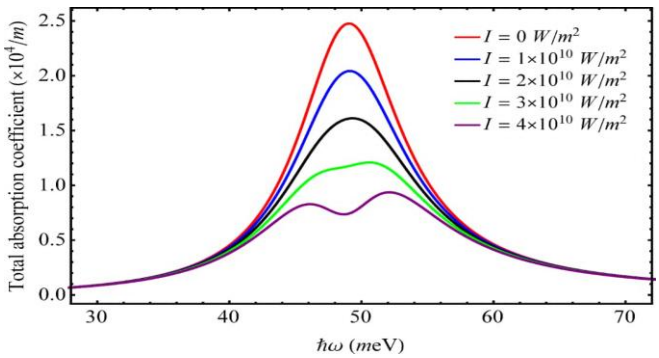

Figure 7 Variation of Total absorption coefficient with photon energy for five different values of optical intensity *I*.

Science World Journal Vol. 20(No 4) 2025 https://dx.doi.org/10.4314/swj.v20i4.44
www.scienceworldjournal.org
ISSN: 1597-6343 (Online), ISSN: 2756-391X (Print)
Published by Faculty of Science, Kaduna State University

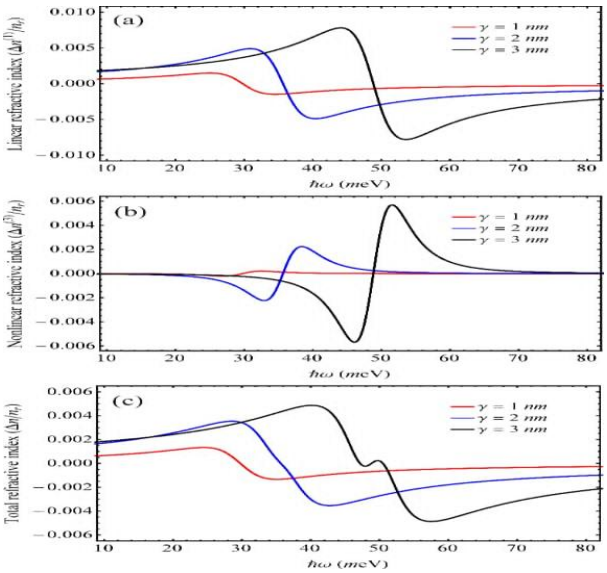

Figure 8 Variation of (a) the linear, (b) third-order nonlinear, and (c) total refractive index changes with incident photon energy for three different values of barrier slope *γ*.

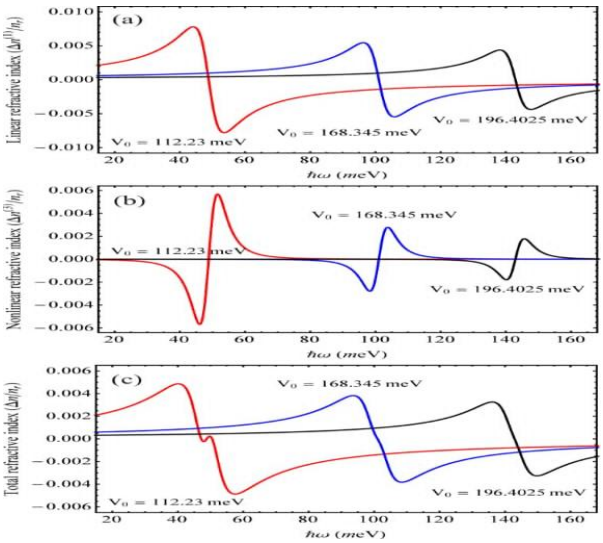

Figure 9 Variation of (a) the linear, (b) third-order nonlinear, and (c) total refractive index changes with photon energy for three different values of barrier height V_0.

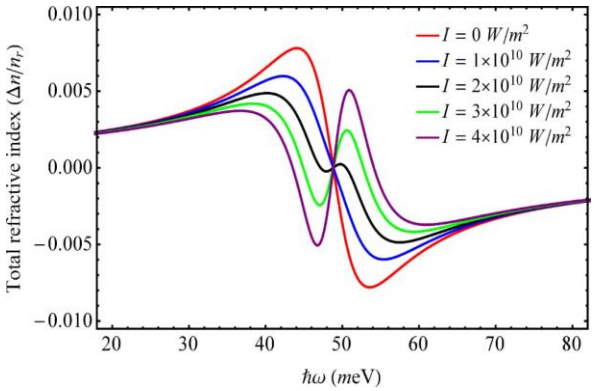

Figure 10 Variation of total refractive index changes with incident photon energy for five different values of the incident optical intensity *I*.

REFERENCES

Ahmadov, A. I., Aslanova, S. M., Orujova, M. S., Badalov, S. V., & Dong, S. H. (2019). Approximate bound state solutions of the Klein-Gordon equation with the linear combination of Hulthén and Yukawa potentials. *Physics Letters A*, *383*(24), 3010-3017.

Ahmadov, H. I., Dadashov, E. A., Huseynova, N. S., & Badalov, V. H. (2021). Generalized tanh-shaped hyperbolic potential: bound state solution of the Schrödinger Equation. *The European Physical Journal Plus*, *136*(2), 1-12.

Ahn, D. & Chuang, S.L. (1987b). Calculation of linear and nonlinear intersubband optical absorptions in a quantum well model with an applied electric field. *J. Quantum Electronics*, *23*, 2196-2201.

Alivisatos, A. P. (1996). Semiconductor Clusters, Nanocrystals, and Quantum Dots. *Science*, *271*(5251), 933–937.

Anchala, Purohit, S.P. & Mathur, K.C. (2012). Effect of barrier height on linear and nonlinear photoabsorption and refractive index in Si quantum dots. Advanced Materials Letters. *3*(6). 498-503.

Antia, A., Ikot, A.N. & Akpabio L. (2010).Exact solutions of the Schrodinger Equation with Manning-Rosen potential plus a Ring-shaped potential by Nikiforov-Uvarov method. *European Journal of Scientific Research*, 45(1), 107-118.

Ashoori, R. . (1996). Electrons in artificial atoms. *Nature*, *379*(6564), 413–419.

Ataser, T., Sonmez, N.A., Ozen, Y., Ozdemir, V., Zeybek, O. & Ozcelik, S. (2018). Developing of dual junction GaI p/GaAs solar cell devices: effects of different metal contacts. *Opt. Quantum Electron.*, *50*, 1-13.

Barati, M., Rezaei, G. & Vahdani, M. . R. . K. (2007). Binding energy of a hydrogenic donor impurity in an ellipsoidal finite-potential quantum dot. *Phys. Status SolidiB*, *244*, 2605-2610.

Baskoutas, S., Paspalakis, E. & Terzis, A. (2006). Effects of excitons in nonlinear optical rectification in semiparabolic quantum dots. Physical Review B, *74*, 153306.

Bhattacharya, P., Ghosh, S., & Stiff-Roberts, A. D. (2004). Quantum dot optoelectronic devices. *Annu. Rev. Mater. Res.*, *34*, 1–40.

Bruchez, M., J., & *et al*. (1998). Semiconductor Nanocrystals as Fluorescent Biological Labels. *Science*, *281*(5385), 2013–2016.

Brus, L. E. (1984). Electron--electron and electron-hole interactions in small semiconductor crystallites: The size dependence of the lowest excited electronic state. *The Journal of Chemical Physics*, *80*(9), 4403–4409.

Cakir, B., Yakar, Y., Cakir, B. & Ozmen, A. (2011). Linear and nonlinear refractive index changes in spherical quantum dot. *Progress in Electromagnetics Research*, *21*, 77-92.

Cecchi, S., Llin, L. F., Etzelstorfer, T., & Samarelli, A. (2015). Review of thermoelectric characterization techniques suitable for SiGe multilayer structures. *The European Physical Journal B*, *88*(3), 1-8.

Chan, W. C., & *et al*. (1998). Quantum Dot Bioconjugates for Ultrasensitive Nonisotopic Detection. *Science*, *281*(5385), 2016–2018.

Chang, C., & Li, X. (2022). Nonlinear optical properties in GaAs/Al0. 3Ga0. 7As quantum dots of inversely quadratic Hellmann plus Kratzer potential. *The European Physical Journal D*, *76*(7), 1-8.

Chen, B., Guo, K.X., Wang, R.Z., Zang, Z.H. & Liu, Z.I. (2009). Linear and nonlinear optical absorption in double triangular quantum wells. *Solid state Commun.*, *149*, 310-314.

Chetouani, L. Guechi & Hammann. (1987). Exact path integral for the ring potential. *Physics Letters A*, *125*(6-7), 277-281.

Chuang, S.L. & Alm, D. (1989). Optical transitions in a parabolic quantum well with an applied electric field—analytical solutions. *J. Appl. Phys*, *65*, 2822.

Coleman, J. J., Young, J. D. & Garg, A. (2011). Semiconductor quantum dot laser: A tutorial. *J Lightwave Tech.*, *29*, 499–510.

Dabbousi, B. O., & *et al*. (1997). (CdSe)ZnS Core-shell Quantum Dots: Synthesis and Characterization of a Size Series of Highly Luminescent Nanocrystallites. *Journal of Physical Chemistry B*, *101*(46), 9463–9475.

Dai, Y.T., Fan, J.C., Chen, Y.F., Lin, R.M., Lee, S.C. & Lin, H.H. (1997). Temperature dependence of photoluminescence spectra in InAs/GaAs quantum dot superlattices with large thicknesses. *J. Appl. Phys.*, *82*, 4489.

Dave, D.P. (1993). Enhanced refractive index change in asymmetrical quantum wells with an applied electric field. *J. Appl. Phys.*, *74*, 6872

Ee, Y. K., Zhao, H., Arif, R. A., Jamil, M., & Tansu, N. (2008). Self-assembled InGaN quantum dots on GaN emitting at 520nm grown by metalorganic vapor-phase epitaxy. *J. Crystal Growth*, *310*, 2320–2325.

Ehsanfard, N. & Vahdani, M. (2015). Intersubband optical absorption coefficients and refractive index changes in a Gaussian spherical quantum dot. *International Journal of Theoretical Physics*, *54*, 2419-2435.

Franken, P., Hill, A., Peters, C. & Weinreich, G. (1961). Generation of optical harmonics. *Physical Review Letters*, *7*(4), 118-119.

Gao, X., & *et al*. (2004). In vivo cancer targeting and imaging with semiconductor quantum dots. *Nat Biotech*, *22*(8), 969–976.

Gibbs, H.M. (1985). Optical Bistability: Controlling light with light.(Academic Press New York).

Gonul, B. & Zorba, I. (2000). Supersymmetric solutions of non-central potentials. *Physics Letters A, 269*(2-3), 83-88.

Grundmann, M., Bimberg, D. & Ledentsov, N. N. (1998). *Quantum Dot Heterostructures*. Wiley.

Gu, T., Petrone, N., Mcmillan, J.F., Vander Zande, A., Yu, M., Kwong, D.L., Hone, J. & Wong, C.W. (2012). Regenerative oscillationand four-wave mixing in graphene optoelectronics. *Nat. Photonics.*, *6*, 554-559.

Gu, X.Y. & Dong, S.H. (2011). Energy spectrum of the Manning-Rosen potential including centrifugal term solved by exact and proper quantization rules. *Journal of Mathematical Chemistry*, *49*, 2053.

Harrison, P. (2005). Theoretical and Computational physics, second Edition, John wiley, New York.

Hendry, E., Hale, P.J., Moger, J., Savechenko, A. & Khailov, S.M. (2010). Coherent nonlinear optical response of graphene. *Phys. Rev. Lett*, *105*, 097401.

Heiss, D., Kroutvar, M., Finley, J. J., & Abstreiter, G. (2005). Progress towards single spin optoelectronics using quantum dot nanostructures. *Solid state communications*, *135*(9-10), 591-601.

Ibrahim, K. & Sotirios, B.. (2008). Linear and nonlinear optical absorption coefficients and refractive index changes in spherical quantum dots. Effects of impurities, electric field, size, and optical intensity. *Journal of Applied Physics*, *103*, 073512.

Ibrahim, K., Unlu, S. & Safak, H. (2006). Linear and nonlinear intersubband optical absorption coefficients and refractive index changes in a quantum box with finite confining potential. *Physica E*, *33*, 319-324.

Ikhdair, S. (2008). Exact solutions of the D-Dimensional Schrödinger equation for a pseudo-coulomb potential plus ring-shaped potential. *Chinese Journal of Physics*, 46(3), 291-306.

Jafari, A.R, & Naimi, Y. (2014). Optical properties of quantum dots versus quantum antidots: Effects of hydrogenic pressure and temperature. *J. Comput Electron*, *13*, 666-672.

Jorge, P. A. S., Mayeh, M., Benrashid, R., Caldas, P., Santos, J. L., & Farahi, F. (2006). Applications of quantum dots in optical fiber luminescent oxygen sensors. *Appl.Opt.*, *45*, 3760–3767.

Kang, G., Yoo, J., Ahn, J., & Kim, K. (2015). Transparent dielectric nanostructures for efficient light management in optoelectronic applications. *Nano Today*, *10*(1), 22-47.

Karimkhani, A., & Moravvej-Farsh, M. K. (2010). Temperature dependence of optical near field energy transfer rate between two quantum dots in nanophotonic devices. *Appl. Opt.*, *49*, 1012–1019.

Khordad, R. & Mirhosseini, B. (2014). Linear and nonlinear optical properties in spherical quantum dots: Rosen morse potential. Optics and spectroscopy. *117*(3), 434-440.

Khordad, R. (2012). Pressure effect on optical properties of modified Gaussian quantum dots. *Physica B*, *407*, 1128-1133.

Khordad, R., Khaneghah, S. K., & Masoumi, M. (2010). Effect of pressure on intersubband optical absorption coefficients and refractive index changes in a V-groove quantum wire. *Superlattices and Microstructures*, *47*(4), 538-549.

Khordad, R., & Mirhosseini, B. (2015). Application of Tietz potential

to study optical properties of spherical quantum dots. *Pramana*, *85*(4), 723-737.

Kirak, M., Yilmaz, S., Sahin, M. & Gencaslan. (2011). The electric field effects on the binding energies and the nonlinear optical properties of a donor impurity in a spherical quantum dot. *J. Appl. Phys.*, *109*, 094309.

Kuhn, K. J., Lyengar, G. U., & S. Yee. (1991). Free carrier induced changes in the absorption and refractive index for intersubband optical transitions in AlxGa1-xAs/GaAs/AlxGa1-xAs quantumwells. *J. Appl. Phys.*, *70*, 5010.

Kurgin, J.B. & Li, S. (1993). Two photon absorption and resonant nonlinear index of refraction in the intersubband transitions in the quantum wells. *Applied physics Letters*, *62*, 126.

Kurtz, S.R. (1999). Nature of the fundamental band gap in GaNxP1−xGaNxP1−x alloys. *Phys. Rev. Lett.*, *82*, 1221.

Larson, D. R., & *et al*. (2003). Water-Soluble Quantum Dots for Multiphoton Fluorescence Imaging in Vivo. *Science*, *300*(5624), 1434–1436.

Lee, C. M., Ruan, W. Y., Li, J. Q., & Lee, R. C. (2005). Magnetic-field dependence of low-lying spectra in magnetic quantum rings and dots. *Physical Review B*, *71*(19), 195305.

Lee, H., Yang, W. & Sercel, P.C. (1996). Temperature and excitation dependence of photoluminescence line shapein InAs/GaAs quantum-dot structures. *Phys. Rev. B, 55*, 9757.

Li, X. C., Wang, A. M., Wang, Z. L., & Yang, Y. (2012). Second-harmonic generation in asymmetric quantum dots in the presence of a static magnetic field. *Chinese Physics B*, *21*(8), 087303.

Li, B., Guo, K.X., Zhang, C.J. & Zhang, Y.B. (2007). The second-harmonic generation in parabolic quantum dots in the presence of electric and magnetic fields. *Phys. Lett. A*, *367*, 493.

Liang, B. L., Wang, Z. M., Mazur, Y. I., & Salamo, G. J. (2006). Photoluminescence of surface InAs quantum dot stacking on multilayer buried quantum dots. *Applied physics letters*, *89*(24), 243124.

Liang, S.J., Xie, W.F. & Shen, H.Y. (2011). Optical properties in a two-dimensional quantum ring: Confinement potential and Aharonov–Bohm effect. *Opt. Commun.*, *284*, 5818.

Lu, L., Xi, W. & Hassanabadi, H. (2011). Linear and nonlinear optical absorption coefficients and refractive index changes in a two-electron quantum dot. *Journal of applied Physics, 109*, 063108.

Lu, L., Xi, W. & Hassanabadi, H.. (2011). The effects of intense laser on nonlinear properties of shallow donor impurities in quantum dots with the woods- saxon potential. *Journal of Luminescence, 131*, 2538-2543.

Luque, A., Marti, A., Antolin, E., & Garcia-Linares, P. (2010). Intraband absorption for normal illumination in quantum dot intermediate band solar cells. *Solar Energy Materials & Solar Cell*, *94*, 2032–2035.

Machavariani, Z.S. (2016). The effects of the optical anisotropy for the system with one electron confined in ellipsoidal potential well. *GEST: Physics, 1*(15) 1461-1512.

Masumoto, Y., & Takagahara, T. (2002). *Semiconductor Quantum Dots*. Springer.

Máthé, L., Onyenegecha, C. P., Farcaş, A. A., Pioraş-Ţimbolmaş, L. M., Solaimani, M., & Hassanabadi, H. (2021). Linear and nonlinear optical properties in spherical quantum dots: Inversely quadratic Hellmann potential. *Physics Letters A*, *397*, 127262.

Michalet, X., & *et al*. (2005). Quantum Dots for Live Cells, in Vivo Imaging, and Diagnostics. *Science*, *307*(5709), 538–544.

Nalwa, H.S. & Miyatta, S. (1997). Nonlinear optics of organic molecules and polymers. CRC press.

Newell, T. C., Bossert, D. J. ., Stintz, A., Fuchs, B., Malloy, K. L., & Lester, L. F. (1999). Gain and Line width Enhancement Factor in InAs Quantum-Dot Laser Diodes. *IEEE Quantum Electron.*, *11*, 1527–1529.

Nikiforov, A.F., Uvarov, V.B., *Special Functions of Mathematical Physics* (Birkhauser, Basel, 1988).

Ntziachristos, V., & *et al*. (2002). Fluorescence molecular tomography resolves protease activity in vivo. *Nat Med*, *8*(7), 757–761.

Onyeaju, M.C., Idiodi, J.O.A., Ikot, A.N., Solaimani, M. & Hassanabadi, H. (2016a). Linear and nonlinear optical properties in spherical quantum dots: Generalized Hulthen Potential. *Few-Body systems*, 57(9), 793-805.

Onyeaju, M.C., Idiodi, J.O.A., Ikot, A.N., Solaimani, M. & Hassanabadi, H. (2016b). Linear and nonlinear optical properties in spherical quantum dots: Manning-Rosen potential. *J. Opt., 46*, 254–264 .

Onyeaju, M. C., & Onate, C. A. (2021). Dielectric effect on the optical properties of exciton quantum dot with Gaussian plus generalized Hulthen potential as Pseudo-Harmonic potential. *The European Physical Journal D*, *75*(1), 1-8.

Onyenegecha, C. P. (2022). Linear and nonlinear optical properties in spherical quantum dots: Modified Möbius squared potential. *Heliyon*, *8*(8), e10387.

Ozmen, A.Y., Yakar, Y., Cakir, B., & Atav, U. (2009). Computation of the oscillator strength and absorption coefficients for the intersubband transitions of the spherical quantum dot. *Opt. Commun.*, *282*, 3999.

Polimeni, A., Patane, A., Henini, M., Eaves, L., & Main, P. C. (1999). Temperature dependence of the optical properties of I n A s/A l y Ga 1− y As self-organized quantum dots. *Physical Review B*, *59*(7), 5064. Pennelli, G. (2015). Top-down fabrication of silicon nanowire devices for thermoelectric applications: properties and perspectives. *The European Physical Journal B*, *88*(5), 1-12.

Perlin, P. Gorczyca, I., Suski, T., Wisnieswki, P. & Lepkowski, S. (2001). Influence of pressure on the optical properties of $In_xGa_{1-x}N$ epilayers and quantum structures. *Physical Review B*, *64*, 115319.

Perlin, P., Iota, V., Weinstein, B. A., Wiśniewski, P., Suski, T., Eliseev, P. G., & Osiński, M. (1997). Influence of pressure on photoluminescence and electroluminescence in GaN/InGaN/AlGaN quantum wells. *Applied physics letters*, *70*(22), 2993-2995.

Qiang, W.C., Zhou, R.S. & Gao, Y. (2007). Any L – state solutions of the Klein-Gordon equation with the generalized Hulthen potential. *Phys. Lett. A*, *372*, 7199.

Radu, A. & Duque, C.A. (2015). Non-linear optical processes involving excited subbands in laser-dressed quantum wires with triangular cross-section. *Physica E*, *72*, 165-

177.

Rahimi, F., Ghaffary, T., Naimi, Y., & Khajehazad, H. (2021). Effect of magnetic field on energy states and optical properties of quantum dots and quantum antidots. *Optical and Quantum Electronics*, *53*(1), 1-16.

Rezaei, G., Vaseghi, B., Taghizadeh, F., Vahdani, M.R.K., & Karimi, M.J. (2010). Intersubband optical absorption coefficient changes and refractive index changes in a two-dimensional quantum pseudodot system. *Superlattices and Microstructures, 48*, 450-457.

Rezaei, G., Vaseghi, B., & Dostimotlagh, N.A. (2012). Linear and nonlinear optical properties of spherical quantum dots. Effects of hydrogenic impurity and conduction band Non-parabolicity. *Commun. Theor. Phys.*, *57*, 485-489.

Rezaei, G., Vahdani, M.R.K. & Vaseghi, B. (2011). Nonlinear optical properties of a hydrogenic impurity in an ellipsoidal finite potential quantum dot. *Current Applied Physics, 11*, 176-181.

Rezaei, G., Vaseghi, B., Taghizadeh, F., Vahdani, M.R.K. & Karimi, M.J. (2010). Intersubband optical absorption coefficient changes and refractive index changes in a two-dimensional quantum pseudodot system. *Superlattices and Microstructures, 48*, 450-457.

Richard, S. (2003). Handbook of Nonlinear Optics. CRC Press.

Rishinaramangalam, A. K., Ul Masabih, S. M., Fairchild, M. N., Wright, J. B., Shima, D. M., Balakrishnan, G., ... & Feezell, D. F. (2015). Controlled Growth of Ordered III-Nitride Core–Shell Nanostructure Arrays for Visible Optoelectronic Devices. *Journal of Electronic Materials*, *44*(5), 1255-1262.

Roan, E.J. & Chuang, S.L. (1991). Linear and nonlinear intersubband electroabsorptions in a modulation-doped quantum well, *J. Appl. Phys.*, 69, 3249.

Sadeghi, E. (2009). Impurity binding energy of excited states in spherical quantum dot. *Physica E*, 41, 1319.

Sedrakian, D.M., Khachatrian, A. Z., Andresyan, G.M. & Badaiyan, V.D. (2004). Second harmonic generation in the symmetric well containing a rectangular barrier. *Optical and Quantum Electronics*, *36*(10), 893-904.

Sauvage, S., Boucaud, P., Glotin, F. & Prazeras, R. (1999). Third-harmonic generation in InAs/GaAs self-assembled quantum dots. *Phys. Rev. B*, *59*, 9830.

Sahin, M. (2008). Photoionization cross section and intersublevel transitions in a one and two electron spherical quantum dot with a hydrogenic impurity. *Phys. Rev. B*, 77, 045317.

Sahin, M. (2009). Third-order nonlinear optical properties of a one and two-electron spherical quantum dot with and without a hydrogenic impurity. *J. Appl. phys.*, *106*, 063710.

Shaller, R.D., Robert, K. S., Jeffrey P.M. & Kirill, Z.. (2007). Optical properties of PbSe nanocrystal quantum dots under pressure. *Applied Physics Letters*, *90*, 043110.

Shao, S., Guo, K. X., Zhang, Z. H., Li, N., & Peng, C. (2010). Studies on the third-harmonic generations in cylindrical quantum dots with an applied electric field. *Superlattices and Microstructures*, *48*(6), 541-549. Shi, L., & Yan, Z. W. (2017). Linear and nonlinear optical properties of an off-center donor in GaAs/AlGaAs and AlGaAs/GaAs core-shell ellipsoidal quantum dots. *Superlattices and Microstructures*, *109*, 382-393.

Smith, S. D. (1986). Optical bistability, photonic logic, and optical computation, *Appl. Opt.*, *25*, 1550-1564.

Suraprapapich, S. ., Thainoi, S., Kanjanachuchai, S., Panyakeow, S. ., & . (2006). Quantum dot integration in hetrostructure solar cell. *Solar Energy & Solar Cells*, *90*, 2968–2974.

Tang, Y., Rich, D. H., Mukhametzhanov, I., Chen, P., & Madhukar, A. (1998). Self-assembled InAs/GaAs quantum dots studied with excitation-dependent cathodoluminescence. *Journal of Applied Physics*, *84*(6), 3342-3348.

Tas, H., & Sahin, M. (2012). The inter-sublevel optical properties of a spherical quantum dot-quantum well with and without a donor impurity. *J. Appl. Phys.*, *112*, 053717

Tezcan, C., & Sever, R. (2009). A general approach for the exact solution of the Schrödinger Equation *Int. J. Theor. Phys.*, *48*, 337.

Teleb, H., Abedi, K., & Golmohammadi, S. (2011). Operation of quantum-dot semiconductor optical amplifiers under nonuniform current injection. *Appl. Opt.*, *50*, 608–617.

Troccoli, M., Belyanin, A., Capasso, F., Kubukcu, E., Sinco, D. L., & Cho, A. Y. (2005). M. Troccoli, A. Belyanin, F. Capasso, E. Kubukcu, D.L. Sinco, A.Y. Cho. *Nature*, *433*(845).

Vahdani, M. R. K., & Rezaei, G. (2009). Linear and nonlinear optical properties of a hydrogenic donor in lens-shaped quantum dots. *Physics Letters A*, *373*(34), 3079-3084.

Vaseghi, B., Rezaei, G. & Sajadi, T. (2015). Optical properties of parabolic quantum dots with dressed impurity: Combined effects of pressure, temperature and laser intensity. *Physical B: Condensed Matter, 4*(56), 171-175.

Vurgaftman, 8., Meyer, J. R., & Ram-Mohan, L. R. (1996). Optimized second-harmonic generation in asymmetric double quantum wells. *IEEE journal of quantum electronics*, *32*(8), 1334-1346.

Wang, G. H., Guo, Q., & Guo, K. X. (2003). Refractive index changes induced by the incident optical intensity in semiparabolic quantum wells. *Chinese journal of physics*, *41*(3), 296-306.

Wang, G. (2005). Third-harmonic generation in cylindrical parabolic quantum wires with an applied electric field. *Phys. Rev. B*, *72*, 155329.

Wang, G. & Guo, Q. (2008). Nonlocal effects on second-harmonic generation in a Poschl-Teller quantum well. *European Physical Journal B*, *63*, 219-225.

Wei, G. F., & Dong, S. H. (2008). Approximately analytical solutions of the Manning–Rosen potential with the spin–orbit coupling term and spin symmetry. *Physics Letters A*, *373*(1), 49-53.

Wu, R., Zhang, Y., Yan, S., Bian, F., Wang, W., Bai, X., Lu, X., Zhao, J., & Wang, E. (2011). Purely coherent nonlinear optical response in solution dispersions of graphene sheets. *Nano Lett.*, *11*, 5159-5164.

Xie, W. (2008). Linear and nonlinear optical properties of a hydrogenic donor in spherical quantum dots. *Physica B*, *403*, 4319-4322.

Yakar, Y., Cakir, B. & Ozmen. (2010a). Optical properties in spherical quantum dots. *Communications in Theoretical Physics*, 53, 1185.

Yan, Z.W., & Shi, L. (2014). Electric field and shape effect on the linear and nonlinear optical properties of ellipsoidal finite potential quantum dots. *Superlattices and Microstructures*, *75*, 503-513.

Yan, Z.W., & Shi, L. (2016). Electric field and shape effect on the linear and nonlinear optical properties of multi-shell ellipsoidal quantum dots. *Superlattices and Microstructures*, *94*, 204-214.

Yao, W., Yu, Z., Liu, Y. & Jia, B. (2009). Linear and nonlinear optical absorption coefficient and refractive index changes in strained GaN/AlN quantum dots. *Physica E*, *41*, 1382-1385.

Yuan, J., Xie, W. & He, I. (2009). An off-center donor and nonlinear absorption spectra of spherical quantum dots. *Physica E*, *41*, 779-785.

Wu, Y. R., Lin, Y. Y., Huang, H. H., & Singh, J. (2009). Electronic and optical properties of InGaN quantum dot-based light emitters for solid state lighting. *Journal of Applied Physics*, *105*(1), 013117. Zhang, L., & Shi, J. J. (2005). Calculation of linear and nonlinear intersubband refractive-index changes in an asymmetrical semiparabolic quantum well with applied electric field. *physica status solidi (b)*, *242*(5), 1001-1009.

Zhang, L. (2005). Electric field effect on the linear and nonlinear intersubband refractive index changes in asymmetrical semiparabolic and symmetrical parabolic quantum wells. *Superlattices Microstruct.*, *37*, 261-272.

Zhang, M. & Guo- Qing. (2010). Exact solution of a new Coulomb ring-shaped potential. *Journal of Mathematical Chemistry*, *48*(14), 876-882.

Zhang, M., Sun, G. & Dong, S. (2010). Exactly complete solutions of the standard Schrödinger equation with a spherically harmonic oscillatory ring-shaped potential. *Physics Letters A*, 374(5), 704-708.